Joint Measurements of Terahertz Wave Generation and High-Harmonic Generation from Aligned Nitrogen Molecules Reveal Angle-Resolved Molecular Structures

Yindong Huang, Chao Meng, Xiaowei Wang, Zhihui Lü, Dongwen Zhang, Wenbo Chen, Jing Zhao, Jianmin Yuan, and Zengxiu Zhao

Phys. Rev. Lett. **115**, 123002 — Published 18 September 2015

DOI: 10.1103/PhysRevLett.115.123002

Angle-resolved molecular structures joint measurements of terahertz wave generation and high harmonic generation from aligned nitrogen molecules

Yindong Huang[1], Chao Meng[1], Xiaowei Wang[1], Zhihui Lü[1], Dongwen Zhang[1], Wenbo Chen[1], Jing Zhao[1], Jianmin Yuan[1,2*] and Zengxiu Zhao[1†]

[1] *Department of Physics, College of Science, National University of Defense Technology, Changsha 410073, Hunan, People's Republic of China*

[2] *IFSA Collaborative Innovation Center, Shanghai Jiao Tong University, Shanghai 200240, People's Republic of China*

(Dated: July 13, 2015)

We report the synchronized measurements of terahertz wave generation and high harmonic generation from aligned nitrogen molecules in dual-color laser fields. Both yields are found alignment-dependent showing the importance of molecular structures in the generation processes. By calibrating the angular ionization rates with the THz yields, we present a new way to retrieve the angular differential photoionization cross section (PICS) from the harmonic signals, which avoids specific model calculations or separate measurements of the alignment-dependent ionization rates. The measured PICS is found consistent with theoretical predications, although some discrepancies exist. This all-optical method provides a new alternative to investigate molecular structures.

PACS numbers: 32.80.Rm 42.50.Hz 42.65.Ky

The recent development of coherent table-top sources of terahertz (THz) waves and soft X-rays delivers a much more comprehensive insight and control on ultrafast dynamics in matter [1–4]. Synchronizing terahertz wave generation (TWG) with high harmonic generation (HHG) has presented a new opportunity peering into the complete electron dynamics in intense laser fields, with time scales spanning 6 orders of magnitudes. A unified picture of TWG and HHG has been drawn. Briefly, liberated electrons from atoms or molecules accumulate energy and may revisit the parent core in the oscillating fields. The re-colliding electrons emit high-order harmonics upon recombination [5]; while the direct escaping and the forward re-scattering electrons contribute to TWG [6, 7].

However on aligned molecules, direct comparisons between TWG and HHG have never been conducted yet. The alignment-dependent HHG has been proved valuable in uncovering many aspects of molecular properties as demonstrated in the tomography imaging of orbitals [8–15] and the studies on collective electron response [16–18] and nuclear motion [19–21]. It is known from the quantitative rescattering (QRS) theory that the third step of HHG can be viewed as the inverse process of photoionization based on the principle of detailed balance [22]. Therefore the angular differential photoionization cross section (PICS) can be constructed from HHG to obtain the information of the molecular structure [23]. But these investigations usually rely on specific calculations or separate measurements of the alignment-dependent ionization rates (AIR). On one hand, the theoretical predictions, based on the molecular strong field approximation (MO-SFA) [24] or the molecular Ammosov-Delone-Krainov theory (MO-ADK) [25], show discrepancies from the experimental AIR results quantitatively (N_2 and O_2) or even qualitatively(CO_2) [26, 27]. On the other hand, it is a challenge to simultaneously obtain the harmonic yields and ionization rates, since HHG requires high particle density ($\sim 10^{17}$ cm^{-3}), far beyond the limitation of typical ionization detection. Given the ionization dependence of TWG [28], it is thus desired using TWG to map the AIR and to calibrate the HHG in one single experiment instead of separated detections of ions or electrons in completely different experimental conditions. Particularly, THz waves can be coherently detected with high signal to noise ratio [29–31].

In this letter, we perform joint measurements on angular TWG and HHG from aligned nitrogen molecules to give a much more reliable and complete descriptions on molecular structures. To our knowledge, it's the first time to determine the alignment-dependent TWG from molecules in dual-color laser fields, which confirms the importance of molecular orbital in radiating THz waves. By assuming that the THz wave amplitude is proportional to the ionization rate for given alignment, we present a new all-optical method to determine the PICSs of molecules from joint measurements. Great consistence is found between the theoretical predictions and experimental results for interested harmonics, in terms of the fundamental shapes and alignment angles of minimum. But still the quantitative discrepancies exist which need further investigations including such as multi-electron effects.

The experimental setup consists of a 790 nm, 25 fs, 1.5 mJ, 1 kHz Ti:sapphire laser system and vacuum chambers for generating and detecting HHG and THz, as shown in Fig. 1. The output beam is split into three pulses for molecule alignment, THz wave and high harmonics generation and THz detection, respectively. The generation pulse passes through a 30 μm β-BBO to produce its second harmonic. The group velocity dispersion of the dual-color field is compensated by a calcite plate

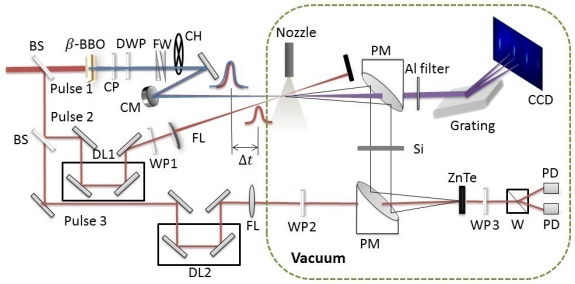

FIG. 1. Experimental setup. BS: beam splitter. CP: calcite plate. DWP: dual wavelength wave plate. FW: fused silica wedges. WP1, WP2: $1/2\lambda$ wave plate. CM: concave mirror. DL: delay line. FL: focusing lens. PM: parabolic mirror. WP3: $1/4\lambda$ wave plate. W: wollaston polarizer. PD: photodiode detector. CH: chopper.

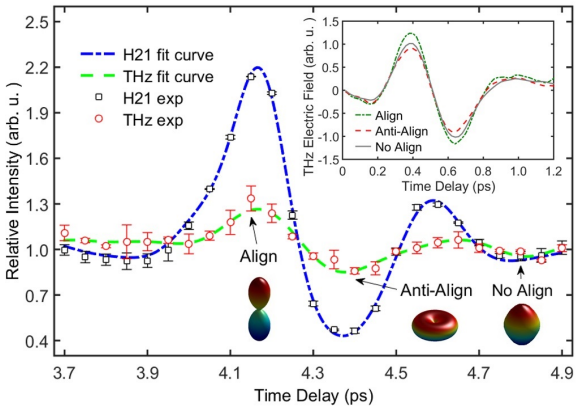

FIG. 2. The modulations of the relative yields of 21st harmonic (black squares) and THz (red circles) as functions of the time delay between alignment and generation pulses with parallel polarization. The blue dash-dotted lines and green dashed lines are the simulations. The inset presents the THz waveforms detected at the moments of alignment, anti-alignment and random alignment indicated by arrows. The corresponding fitted rotational wave packets are illustrated as well.

and their polarizations are rotated to be parallel with a dual wavelength wave plate followed by a pair of fused silica wedges to precisely adjust the relative phase between the dual-color field. Delay line 1 (DL1) is introduced to control the time delay between the alignment pulse and the generation pulse. A rotatable half wave plate (WP1) is inserted to adjust the alignment angle. A beam shutter is also placed to turn on/off the alignment pulse. The generation pulse and alignment pulse are focused ∼0.2 mm below and 2 mm before the orifice of the continuous nozzle (0.2 mm in diameter), which generates a supersonic expansion with 1 bar backing pressure. The intensity of the alignment and the generation pulse is about 0.7×10^{14} W/cm^2 and 1.5×10^{14} W/cm^2, respectively. The THz detection pulse and the TWG are collinearly focused through a 1 mm thick (110)-cut ZnTe crystal for electro-optic sampling (EOS) the THz waveform by varying delay line 2 (DL2). The harmonics pass through a hole-drilled off-axis parabolic mirror (PM1) and are simultaneously recorded by a homemade X-ray spectrometer containing a flat field grating (Hitachi) and a CCD camera (Princeton Instruments). The maximum of THz field strength is estimated to be 35 V/cm.

In the experiment, we kept the cut-off at harmonic order 25th in order to avoid the contributions from the lower lying orbitals mentioned in [13, 32]. Limited to the size of CCD camera, we recorded only the harmonics from order 21st to 25th. The two-color pulses are used to efficiently generate THz waves [33] and their relative phase was optimized by maximizing the THz yields. We observed that the normalized alignment-dependence of odd harmonics shows no significant change when varying the relative phase between dual-color fields, while the situation on the yields of even harmonics was much more complicated. In this letter, we focus on the results of odd harmonics and TWG.

The HHG and the TWG are recorded at different time delays around the half-revival moment (∼ 4.1 ps) of nitrogen molecules, as shown in Fig. 2. The alignment and generation pulses are parallel to each other in polarization. We use supersonic gas jet to deliver pure nitrogen molecules and to minimize the plasma effect, which is different from previous experiments conducted in air [28, 34, 35]. To estimate the degrees of alignment, we compute the rotational wave packet of nitrogen molecules [36, 37]. The simulation parameters are estimated from our experiment conditions and fine adjusted to best fit the experimental data with the least square method. The most suitable rotational temperature is 100 K ± 5 K and the maximum of $\langle\cos^2\theta\rangle$ is about 0.6. The wave packet of the nitrogen has been sketched in Fig. 2 at alignment and anti-alignment moments. We can observe significant modulations of both the THz and the harmonic signals with the evolution of the rotational wave packet. Both signals are the relative yields from the aligned molecules to the random ones achieved by opening or closing the shutter.

The inset of Fig. 2 shows the typical THz wave forms detected by the EOS technique at different time delays. It can be seen that the peak THz amplitude in the case of alignment is much larger than that of anti-alignment, while that from unaligned molecules is in the middle.

After tracing the evolution of HHG and TWG, the rotational wave packet of nitrogen can be reconstructed at any time delay. Then we keep the polarization of generation pulse fixed and rotate the WP1 to acquire the alignment-dependent TWG and HHG. In Fig. 3, we present the angular distributions of THz and the 23rd harmonic yields from experiments at the alignment and anti-alignment moments. In fact, the measured signal $M(\alpha', t_D)$ at the time-delay t_D (DL1) is a convolution

of the single molecule response $S(\theta)$ with the alignment distribution $\rho(\theta', t_{\rm D})$ [26]. Here we have assumed that the measured signals are the incoherent sum of the single molecular yields from all solid angles [38],

$$M(\alpha', t_{\rm D}) = \frac{1}{8\pi^2}\int_0^{2\pi} d\varphi' \int_0^{\pi} d\theta' S\left[\theta(\theta', \varphi'; \alpha')\right] \times \rho(\theta', t_{\rm D}) \sin\theta'. \quad (1)$$

The variable θ is the angle between the polarization axis of generation pulse and internuclear axis. The variable θ' (φ') is the polar (azimuthal) angle in the frame about the polarization axis of the aligning pulse. α' represents the angle between the polarization axis of the alignment and generation pulse. We use the primed notations for the laboratory frame and the unprimed notations for the molecular frame. In order to obtain the alignment-dependent THz and harmonic yields in the molecular frame, deconvolution can be performed from the measurements at either the alignment or anti-alignment moments by expanding $S(\theta)$ in Legrand polynomials [26]. As the advantage of the present joint measurements, both the THz and harmonic yields as functions of alignment angle can be retrieved simultaneously shown in the right column of Fig. 3. Based on the error propagation analysis, the relative standard deviations are found to be 3.2% and 5.9% for HHG and TWG respectively.

For comparison, we also present the calculated angular ionization probabilities based on the MO-ADK theory using the same laser intensity [25]. The similar shapes imply that the alignment-dependence of ionization rates, the THz yields, and harmonic yields are all closely associated to the electronic structure of HOMO. The joint measurements of TWG and HHG allow us to obtain the PICS at different harmonic orders without prior knowledge of alignment-dependence of the ionization rate as demonstrated below.

According to the residual current model [28, 39] for THz generation in dual-color field, the amplitude of TWG field can be written as

$$E_{\rm THz}(t,\theta) \propto \frac{d\langle J(t,\theta)\rangle}{dt} \approx \langle e v_{\rm d}(t) N(t,\theta)\rangle, \quad (2)$$

where J represents the directional current, e is the electron charge, $v_{\rm d}(t)$ represents the drift velocity of electron born at t, and N represents the quantity of ionized electron at t. The drift velocity is dominantly affected by the combined Coulomb field and the laser fields. By fixing the delay between the dual-color fields, the angular THz amplitude is proportional to the time-integrated AIR. Therefore the angular TWG are capable of describing the angular ionization properties in aligned molecules, which gives a more comprehensive picture of the generating mechanism. This method exhibits the convenience to acquire sufficient information about the strong field process without changing the experiment conditions, such as laser intensity or gas density.

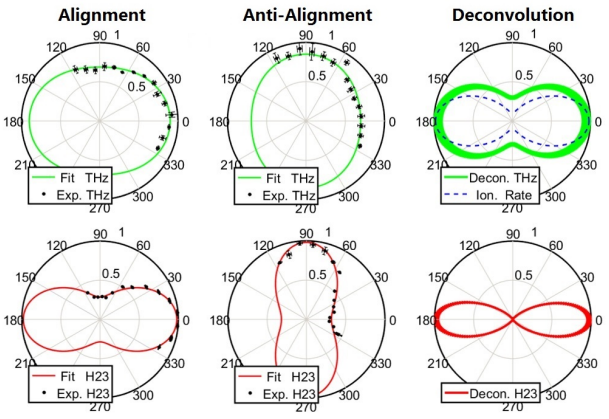

FIG. 3. Alignment-dependent TWG and HHG and their deconvoluted single molecular responses. Left and middle columns show the experimental (black solid circles) and theoretical (green and red solid curves) results of the angular TWG (up) and HHG (down) at alignment and anti-alignment moments respectively. The retrieved molecular frame THz wave (green solid lines) and harmonic yields (red solid lines) are shown in the right column with relative standard deviations indicated by the width of lines. The calculated ionization rates (blue dashed lines) are presented as well.

The angular harmonic intensity $I(\omega,\theta)$ is given by[22]

$$I(\omega,\theta) \propto \omega^4 D^2(\omega,\theta), \quad (3)$$

with $D(\omega,\theta) = W(\omega)\, d(\omega,\theta)\, N(\theta)^{1/2}$. Here $W(\omega)$ is the microscopic wave packet and $d(\omega,\theta)$ is the recombination dipole moment proportional to the square root of the PICS. By treating the AIR as the angular THz amplitude [28], Eq. (3) can be rewritten as follows:

$$I(\omega,\theta) \propto \omega^4 W^2(\omega)\, \sigma_{\rm PICS}(\omega,\theta) \sqrt{I_{\rm THz}(\theta)}. \quad (4)$$

In the right side of Eq. (4), the first two items, only associated to the frequency of harmonics, can be neglected when comparing the alignment dependence of particular harmonic order. Therefore the amplitude of angular PICS can be expressed by using the deconvolution results from the experiments,

$$\sigma_{\rm PICS}(\omega,\theta) \propto \frac{I_{\rm HHG}(\omega,\theta)}{\sqrt{I_{\rm THz}(\theta)}}. \quad (5)$$

In Fig. 4, we show the deduced PICS of different harmonics from the measurements using Eq. (5). We emphasize that the harmonic cut-off is harmonic order 25th, and the electrons from HOMO dominate the process of HHG. The experimental results are compared to the theoretical differential PICS from HOMO of nitrogen molecules [18], which exhibits a good consistency in general. From harmonic order 21st to 25th, the alignment angle of PICS's minimum is gradually shifting to larger angles, which is observed in both experimental and theoretical results.

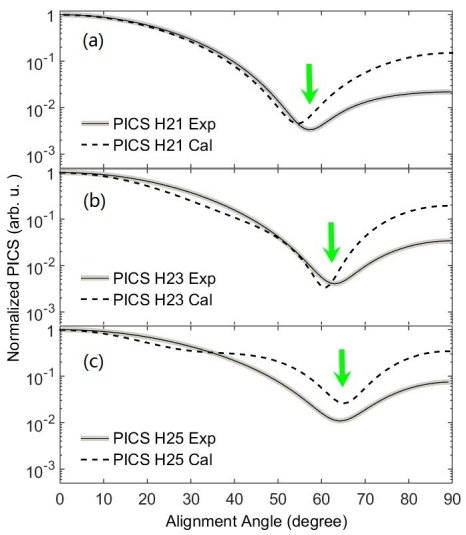

FIG. 4. The normalized theoretical (dashed line) and experimental (solid line) photoionization cross section of harmonic order 21st (a), 23rd (b) and 25th (c) as functions of alignment. The grey areas along the experimental results depict the relative standard deviations estimated from error transferring. The theoretical results are calculated by QRS theory. The green arrows indicate the gradually shifting of minimums.

The minimums reflect the sign changes of the transition dipole matrix element around the corresponding angles which are closely associated with molecular structures. Assuming only the HOMO orbital is involved, the minimum can be considered as the two-center destructive interference of the transitions from the individual atoms [40]. However, in term of the linear combination of atomic orbitals, the coefficients in the HOMO of N_2 for the s component are in phase, while those for the p_z component are out of phase. Therefore the phase difference of the two paths of recombination are complicated with additional phase shift $\Delta\phi$ depending on the relative amplitudes into either s or p_z orbitals [41]. Roughly, the angle at the minimum can be determined by the destructive interference condition as $kR\cos\theta = \pi - \Delta\phi$, where k is the wave number of the electron wave at given harmonic order, R is the internuclear distance and θ is the alignment angle. Since $\Delta\phi$ varies little from the 21st to 25th harmonics, the angle at minimum is increased as k is increasing, qualitatively in agreement with the experimental observation and the numerical calculation [18]. It thus implies that accurate retrieval of the differential PICS is a must for better description of molecular orbital.

We note that there still exists some discrepancies between the experimentally deduced and the theoretically calculated PICS around and beyond the angles at the minimum. Taking the 25th harmonic as an example, the PICS retrieved from the experiment is lower than the theoretical calculation from 30 to 90 degrees. Recently, the theoretical investigation on TWG from molecules has pointed out that the alignment dependence does not strictly follow the square of AIR [42], however the differences are too small to interpret the pronounced suppression. As mentioned previously, the direct ionization of the lower orbitals can be ruled out in this work because of the applied low laser intensity. But as indicated in [43–45], the multi-electron effects could still contribute though dynamical core polarization and distortion of the HOMO orbitals during the interaction of N_2 molecules with the laser field. It means that HOMO-1 could contribute to HHG through anti-screening the HOMO electrons, especially when the field is perpendicular to the molecular axis. This explains why the discrepancies are small when the field are parallel to the molecular axis, while it is pronounced at the perpendicular alignment. In order to verify this claim, different wavelength might be used to explore the dynamic polarization effects. The other possible reason is that the single electron approximation is used in the theoretical calculation of the PICS from the HOMO [46]. It is known that single configuration Hartree-Fock theory fails in obtaining the correct ordering of HOMO-1 and HOMO of nitrogen molecules.

In summary, we demonstrate the synchronized measurements on TWG and HHG from aligned N_2 molecules. Different from previous experiment that using HHG to gauge THz generation [6], here we use THz generation to calibrate the ionization process in HHG and obtain the angular differential PICS through deconvolution of harmonic signals. This new approach saves separate measurements of ionization rates and takes the advantage of coherent THz wave detection, and therefore gives more reliable results as indicated in the clearly resolved minimum of PICS. Qualitative agreement with theoretical calculations is reached, although quantitative discrepancies exist around and beyond the angles where harmonic yields take minimum. We suggest that further theoretical and experiment investigations should consider multi-electron effects involved in HHG from aligned nitrogen molecules. We also expect that TWG is further exploited to better characterize ionization as well as HHG of other molecules.

This work is supported by the National Basic Research Program of China (973 Program) under Grant No. 2013CB922203, and the NSF of China (Grants No. 11374366 and 11474359). The author acknowledges Dr. Cheng Jin for providing his calculating results.

* jmyuan@nudt.edu.cn
† zhao.zengxiu@gmail.com

[1] F. Krausz and M. Ivanov, Rev. Mod. Phys. **81**, 163 (2009).
[2] O. Schubert, M. Hohenleutner, F. Langer, B. Urbanek, C. Lange, U. Huttner, D. Golde, T. Meier, M. Kira,

K. W. Koch, and R. Huber, Nat. Photon. **8**, 119 (2014).
[3] O. Kfir, P. Grychtol, E. Turgut, R. Knut, D. Zusin, D. Popmintchev, T. Popmintchev, H. Nembach, J. M. Shaw, A. Fleischer, H. Kapteyn, M. Murnane, and O. Cohen, Nat. Photon. **9**, 99 (2015).
[4] A. Ferré, A. E. Boguslavskiy, M. Dagan, V. Blanchet, B. D. Bruner, F. Burgy, A. Camper, D. Descamps, B. Fabre, N. Fedorov, J. Gaudin, G. Geoffroy, J. Mikosch, S. Patchkovskii, S. Petit, T. Ruchon, H. Soifer, D. Staedter, I. Wilkinson, A. Stolow, N. Dudovich, and Y. Mairesse, Nat. Commun. **6**, 5952 (2015).
[5] P. B. Corkum, Phys. Rev. Lett. **71**, 1994 (1993).
[6] D. Zhang, Z. Lü, C. Meng, X. Du, Z. Zhou, Z. Zhao, and J. Yuan, Phys. Rev. Lett. **109**, 243002 (2012).
[7] Z. Lü, D. Zhang, C. Meng, X. Du, Z. Zhou, Y. Huang, Z. Zhao, and J. Yuan, Journal of Physics B: Atomic, Molecular and Optical Physics **46**, 155602 (2013).
[8] J. Itatani, J. Levesque, D. Zeidler, H. Niikura, H. Pepin, J. C. Kieffer, P. B. Corkum, and D. M. Villeneuve, Nature (London) **432**, 867 (2004).
[9] T. Kanai, S. Minemoto, and H. Sakai, Nature (London) **435**, 470 (2005).
[10] W. Boutu, S. Haessler, H. Merdji, P. Breger, G. Waters, M. Stankiewicz, L. J. Frasinski, R. Taieb, J. Caillat, A. Maquet, P. Monchicourt, B. Carre, and P. Salieres, Nat. Phys. **4**, 545 (2008).
[11] B. K. McFarland, J. P. Farrell, P. H. Bucksbaum, and M. Gühr, Science **322**, 1232 (2008).
[12] O. Smirnova, Y. Mairesse, S. Patchkovskii, N. Dudovich, D. Villeneuve, P. Corkum, and M. Y. Ivanov, Nature (London) **460**, 972 (2009).
[13] S. Haessler, J. Caillat, W. Boutu, T. Ruchon, T. Auguste, Z. Diveki, P. Breger, A. Maquet, B. Carré, R. Taïeb, and P. Salières, Nat. Phys. **6**, 200 (2010).
[14] C. Vozzi, M. Negro, F. Calegari, G. Sansone, M. Nisoli, S. De Silvestri, and S. Stagira, Nat. Phys. **7**, 822 (2011).
[15] H. Yun, K.-M. Lee, J. H. Sung, K. T. Kim, H. T. Kim, and C. H. Nam, Phys. Rev. Lett. **114**, 153901 (2015).
[16] H. J. Wörner, J. B. Bertrand, P. Hockett, P. B. Corkum, and D. M. Villeneuve, Phys. Rev. Lett. **104**, 233904 (2010).
[17] J. B. Bertrand, H. J. Wörner, P. Hockett, D. M. Villeneuve, and P. B. Corkum, Phys. Rev. Lett. **109**, 143001 (2012).
[18] C. Jin, J. B. Bertrand, R. R. Lucchese, H. J. Wörner, P. B. Corkum, D. M. Villeneuve, A.-T. Le, and C. D. Lin, Phys. Rev. A **85**, 13405 (2012).
[19] N. L. Wagner, A. Wüest, I. P. Christov, T. Popmintchev, X. Zhou, M. M. Murnane, and H. C. Kapteyn, Proceedings of the National Academy of Sciences **103**, 13279 (2006).
[20] J. Zhao and Z. Zhao, Phys. Rev. A **78**, 53414 (2008).
[21] H. J. Worner, J. B. Bertrand, D. V. Kartashov, P. B. Corkum, and D. M. Villeneuve, Nature (London) **466**, 604 (2010).
[22] A.-T. Le, R. R. Lucchese, S. Tonzani, T. Morishita, and C. D. Lin, Phys. Rev. A **80**, 13401 (2009).
[23] X. Ren, V. Makhija, A.-T. Le, J. Troß, S. Mondal, C. Jin, V. Kumarappan, and C. Trallero-Herrero, Phys. Rev. A **88**, 043421 (2013).
[24] T. K. Kjeldsen and L. B. Madsen, Phys. Rev. A **71**, 23411 (2005).
[25] X. M. Tong, Z. X. Zhao, and C. D. Lin, Phys. Rev. A **66**, 33402 (2002).
[26] D. Pavičić, K. F. Lee, D. M. Rayner, P. B. Corkum, and D. M. Villeneuve, Phys. Rev. Lett. **98**, 243001 (2007).
[27] V.-H. Le, N.-T. Nguyen, C. Jin, A.-T. Le, and C. D. Lin, Journal of Physics B: Atomic, Molecular and Optical Physics **41**, 085603 (2008).
[28] Y. S. You, T. I. Oh, A. B. Fallahkhair, and K. Y. Kim, Phys. Rev. A **87**, 35401 (2013).
[29] P. Smith, D. Auston, and M. Nuss, Quantum Electronics, IEEE Journal of **24**, 255 (1988).
[30] J. Dai, X. Xie, and X.-C. Zhang, Phys. Rev. Lett. **97**, 103903 (2006).
[31] Z. Lü, D. Zhang, C. Meng, L. Sun, Z. Zhou, Z. Zhao, and J. Yuan, Applied Physics Letters **101**, 081119 (2012).
[32] Z. Diveki, R. Guichard, J. Caillat, A. Camper, S. Haessler, T. Auguste, T. Ruchon, B. Carré, A. Maquet, R. Taïeb, and P. Salières, Chemical Physics **414**, 121 (2013).
[33] D. J. Cook and R. M. Hochstrasser, Opt. Lett. **25**, 1210 (2000).
[34] J. Wu, Y. Tong, M. Li, H. Pan, and H. Zeng, Phys. Rev. A **82**, 53416 (2010).
[35] T.-J. Wang, S. Yuan, Z.-D. Sun, C. Marceau, Y. Chen, F. Théberge, M. Châteauneuf, J. Dubois, and S. L. Chin, Laser Physics Letters **8**, 295 (2011).
[36] J. Ortigoso, M. Rodríguez, M. Gupta, and B. Friedrich, The Journal of Chemical Physics **110**, 3870 (1999).
[37] Z. X. Zhao, X. M. Tong, and C. D. Lin, Phys. Rev. A **67**, 043404 (2003).
[38] K. Yoshii, G. Miyaji, and K. Miyazaki, Phys. Rev. Lett. **106**, 13904 (2011).
[39] K. Y. Kim, A. J. Taylor, J. H. Glownia, and G. Rodriguez, Nat. Photon. **2**, 605 (2008).
[40] M. Lein, N. Hay, R. Velotta, J. P. Marangos, and P. L. Knight, Phys. Rev. A **66**, 023805 (2002).
[41] B. Zimmermann, M. Lein, and J. M. Rost, Phys. Rev. A **71**, 033401 (2005).
[42] W. Chen, Y. Huang, C. Meng, J. Liu, Z. Zhou, D. Zhang, J. Yuan, and Z. Zhao, arXiv:1503.07588 [physics.atom-ph] (2015).
[43] B. Zhang, J. Yuan, and Z. Zhao, Phys. Rev. Lett. **111**, 163001 (2013).
[44] B. Zhang, J. Yuan, and Z. Zhao, Phys. Rev. A **90**, 035402 (2014).
[45] Z. Zhao and J. Yuan, Phys. Rev. A **89**, 023404 (2014).
[46] R. R. Lucchese, G. Raseev, and V. McKoy, Phys. Rev. A **25**, 2572 (1982).